BEAM LOSS MEASUREMENTS FOR RECURRING FAST LOSS EVENTS DURING 2017 LHC OPERATION POSSIBLY CAUSED BY MACROPARTICLES

A. Lechner*, B. Auchmann, E. Bravin, A. Gorzawski, L. Grob, E.B. Holzer, B. Lindstrom,
T. Medvedeva, D. Mirarchi, R. Schmidt, M. Valette, D. Wollmann, CERN, Switzerland

Abstract

The availability of the LHC machine was adversely affected in 2017 by tens of beam aborts provoked by frequent loss events in one standard arc cell (16L2). In most of the cases, the dumps were triggered by concurrently developing fast beam instabilities leading to particle losses in the betatron cleaning insertion. Many of the events started with a distinct sub-millisecond loss peak comparable to regular dust particle events, which have been observed along all the LHC since the start-up. In contrast to regular dust events, persistent losses developed in cell 16L2 after the initial peaks which can possibly be explained by a phase transition of macroparticles to the gas phase. In this paper, we summarize the observed loss characteristics such as spatial loss pattern and time profiles measured by Beam Loss Monitors (ionization chambers). Based on the measurements, we estimate the energy deposition in macroparticles and reconstruct proton loss rates as well as the gas densities after the phase transition. Differences between regular dust events and events in 16L2 are highlighted and the ability to induce magnet quenches is discussed.

INTRODUCTION

The LHC is the first storage ring with positively charged beams where beam loss events attributed to macroparticles have caused perceivable perturbations of machine operation [1–8]. Since the start-up of the LHC, macroparticle-induced events gave rise to tens of beam aborts and magnet quenches. In addition, several thousand events below dump threshold are observed every year. The events occur in all regions of the LHC rings and manifest themselves as transient loss spikes observed by Beam Loss Monitors (BLM). Because of the ionising energy loss of beam protons traversing a macroparticle, macroparticles get increasingly charged along their passage through the transverse beam tails and are repelled before reaching the beam core. Most of the events observed in the LHC terminate after a few turns (<1 msec).

A new type of loss events was observed in 2017 in one arc cell (16L2) located in sector 12 [9,10]. About two-thirds of the events in 16L2 started with a more or less pronounced loss spike typically lasting for up to a few hundreds of μsec. The spikes resembled regular macroparticle events, but were followed by long loss tails (see Fig. 1) which cannot be caused by solid obstacles because of the high charging rate and the repelling force exerted by the beam. The most likely hypothesis is that the macroparticles in 16L2 heat up suffi-

ciently such that they are subject to a phase transition to the gas phase. In cases, where no distinct loss peak was visible, the macroparticles were possibly undergoing a change of phase before being repelled. In all events, the beams were dumped by BLMs after a duration up to a few hundreds of msec (in one case up to one second). Many of the dumps occurred in the betatron cleaning insertion because of transverse beam instabilities which concurrently developed with the losses in 16L2 [11]. In total, 68 dumps related to 16L2 were observed throughout the year. In one case, the loss-induced particle showers led to a dipole quench in 16L2.

The likely cause of the events in 16L2 was the presence of solid nitrogen (and oxygen) in the vacuum chamber due to accidental air inflow during the end-of-the-year shutdown in 2016 [9,10]. The events in 16L2 were the first macroparticle events in the LHC where a possible phase transition was observed. Regular macroparticle events are believed to be caused by micrometer-sized obstacles or dust introduced during the manufacturing or assembly of magnets and other equipment. The required energy deposition density to induce a phase transition of such obstacles or dust is much higher than for solid nitrogen macroparticles.

This paper presents an analysis of beam-macroparticle interactions in 16L2 based on BLM measurements and parti-
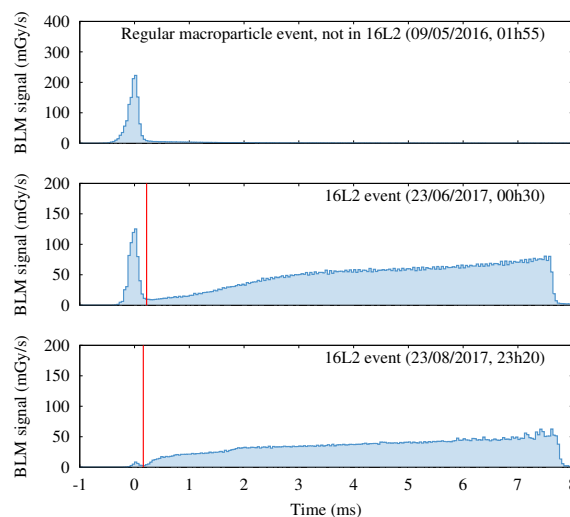

Figure 1: Typical time profile of a regular macroparticle-induced loss event (top) and of two events observed in cell 16L2 (center and bottom). In the two latter cases, solid macroparticles (left of the red line) are possibly subject to a phase transition to the gas phase, which leads to long loss tails (right side of the red line).

* Anton.Lechner@cern.ch

04 Hadron Accelerators

A24 Accelerators and Storage Rings, Other

cle shower simulations with the FLUKA code [12, 13]. The paper provides estimates of the macroparticle size, the energy deposition in the macroparticles, beam-gas collision rates and the gas density after phase transition, and it discusses macroparticle-induced quenches. Other aspects of 16L2 events, such as the impact on LHC availability and the measures taken to improve the operational performance are presented in an accompanying paper [10]. More details about the resulting beam instabilities and about the macroparticle dynamics can be found in Refs. [11, 14, 15].

INELASTIC PROTON COLLISIONS AND ESTIMATED MACROPARTICLE SIZE

The dose measured by BLMs is directly proportional to the number of inelastic collisions N_i of beam protons with nuclei of the macroparticle (or nuclei of the gas after the phase transition). The proportionality factor can be determined empirically using particle shower simulations. This requires a good knowledge of the primary vertices since BLM signals depend on the distance to the loss location. Figure 2 compares measured and simulated BLM patterns for 16L2 events at 6.5 TeV. All patterns are normalized to the maximum signal. The BLM patterns for different events have a strong resemblence to each other, which indicates that the primary vertices were similar in all cases. The measured patterns are well reproduced by the simulation model.

Using the simulated BLM response, it is found that in most events about $1 \times 10^5 - 2 \times 10^6$ of protons had an inelastic collision during the initial loss peak, i.e. during the period where the macroparticle is still believed to have been solid. In a few cases, the initial peak was more pronounced and the number of collisions exceeded 10^7. Assuming that the macroparticles are composed of nitrogen with a density of ρ=0.85 g/cm^3, macroparticle dynamics simulations with the model described in Ref. [16] suggest that the radius needs to be about 15-25 μm to produce $N_i=10^5$ collisions, about 30-50 μm to produce $N_i=10^6$ collisions, and about 50-90 μm to reach $N_i=10^7$ (see Fig. 3). These numbers are only indicative since the effective density of the macroparticle might differ from the assumed value (e.g. frost has a smaller density).
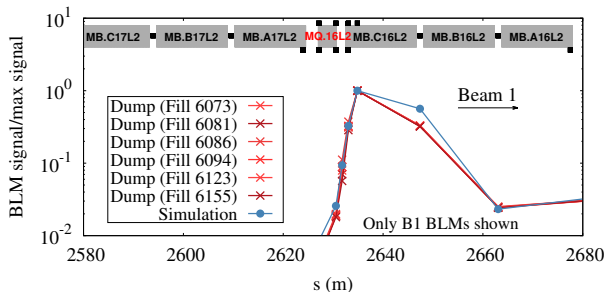

Figure 2: Measured and simulated BLM patterns for beam loss events in 16L2 at 6.5 TeV. In the simulation (blue), point-like losses were assumed in the magnet interconnect between MQ.16L2 and MB.C16L2.
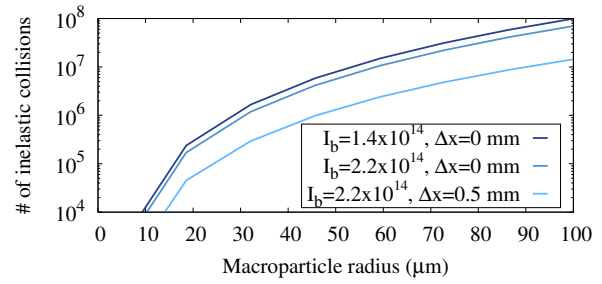

Figure 3: Simulated number of inelastic proton-nucleus collisions in a nitrogen macroparticle with ρ =0.85g/cm^3 versus the macroparticle radius. The curves correspond to different beam intensities I_b and different transverse offsets Δx of the macroparticle with respect to the beam center.

ENERGY DEPOSITION IN NITROGEN MACROPARTICLES

The energy deposited in a macroparticle is determined by the ionising energy loss of beam protons traversing the macroparticle during its passage through the beam. Because of the small macroparticle size, the energy deposition can be approximated as

$$E_d \approx N_p l_{av} S_\Delta, \qquad (1)$$

where N_p is the number of impacting protons, l_{av} is the average path length of protons in the macroparticle, and S_Δ is the restricted stopping power, which includes energy transfers up to Δ. Electrons with kinetic energies higher than Δ are assumed to escape from the macroparticle and deposit their energy elsewhere. Although N_p and l_{av} are *a priori* unknown, their product can be estimated from the number of nuclear collisions derived in the previous section. Nuclear collisions yield only a negligible contribution to the energy deposition in the macroparticle, but their occurence depends also on the number of impacting protons and the average path length. Since the inelastic scattering length $\lambda = M/\rho N_A \sigma$ of high energy protons in solid nitrogen is much larger (tens of cm) than the estimated macroparticle size, N_i can be approximated as:

$$N_i \approx N_p \frac{l_{av} \rho N_A \sigma}{M}, \qquad (2)$$

where ρ is the macroparticle density, M is the molar mass, N_A is the Avogadro constant, and σ is the inelastic proton-nucleus cross section (about 300 mb for collisions of beam protons with nitrogen nuclei). Inserting Eq. (2) into Eq. (1), one gets:

$$E_d \approx N_i \frac{M}{\rho N_A \sigma} S_\Delta. \qquad (3)$$

Assuming Δ=30 keV ($S_\Delta/\rho \approx 1.4$ MeV/g/cm^2), Eq. (3) gives an energy deposition of $E_d \approx 2 \times 10^n$ μJ for $N_i=10^{5+n}$ collisions. Using the estimated macroparticle mass from the previous section, one finds that dose values between a few tens and a few hundreds of J/g are reached. Such dose values lead to a temperature rise of a few tens of K, which is

sufficient to induce a phase transition if one assumes that the initial macroparticle temperature was similar to the beam screen temperature (5-20 K).

GAS DENSITY AFTER PHASE TRANSITION

The theoretical description of the phase transition due to the shock-heating and the subsequent gas expansion would require more complex modelling approaches, which are beyond the scope of this paper. The gas density after the phase transition can, however, be estimated from the beam-gas collision rate dN_i/dt reconstructed from BLM signals. Assuming for simplicity that the gas density is constant over a length L and zero otherwise, the collision rate and atom density $n_a = \rho N_A/M$ of a monoatomic gas are related according to the following equation:

$$\frac{dN_i}{dt} = I_b f_r L n_a \sigma, \qquad (4)$$

where I_b is the circulating beam intensity, f_r is the LHC revolution frequency (11245 Hz). The longitudinal expansion L of the gas is unknown and remains a free parameter. The measured BLM patterns exhibited only a small variation throughout events, which suggests that beam-gas collisions were restricted within a few meters of the original loss location. More simulation studies are needed to confirm this assumption. Figure 4 shows the average beam-gas collision rate and the estimated nitrogen gas density for different 16L2 events, assuming different expansion lengths between $L = 10$ cm and $L = 3$ m. In most events, the average collision rate was around 10^{10} s^{-1} and the estimated gas density between 10^{19} and 10^{22} depending on L. This shows that a macroparticle phase transition can lead to a sudden pressure bump where the atom density is at least 4-5 magnitudes higher compared to the regular residual gas in the arcs.
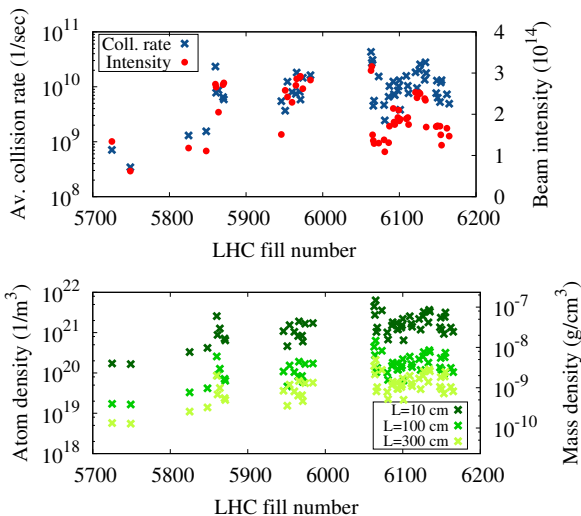

Figure 4: Average proton collision rate (top) and estimated nitrogen gas density (bottom) for different 16L2 events.
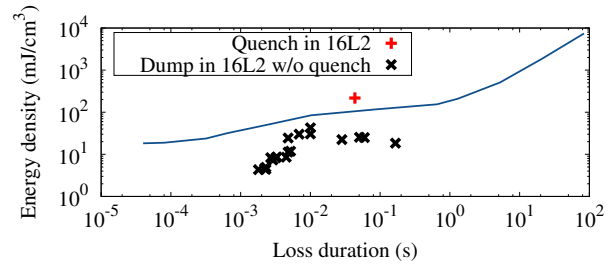
Figure 5: Reconstructed maximum energy density in dipole coils for different 16L2 loss events at 6.5 TeV versus the loss duration. Only events for Beam 1 are shown. The solid line represents quench levels from Ref. [17].

MAGNET QUENCHES

Experience from LHC Run 2 showed that macroparticle-induced losses can quench superconducting dipoles in the LHC arcs [6, 8]. Before the occurrence of 16L2 events in 2017, a total of six dipole quenches attributed to macroparticles were observed during operation at 6.5 TeV. Macroparticles in 16L2 would not have had the potential to induce a quench if no phase transition would have occurred. All 16L2 events with the exception of one were terminated by BLMs without leading to a quench. In one case, however, BLM signals remained just below dump thresholds and a quench occurred after 45 msec because of beam-gas collisions.

Figure 5 compares the estimated maximum energy density in dipole coils for different 16L2 loss events at 6.5 TeV against quench levels implemented in BLM threshold settings [17]. The energy density in the coils was reconstructed with shower simulations using the estimates for N_i. The quench levels derive from the QP3 code [18] and incorporate empirical corrections from quench tests carried out in LHC Run 1 [19]. The obtained energy densities are compatible with the observed quench and the absence of quenches in all other cases. The results also illustrate that in a few other events the energy density was only a factor of 2–3 below the quench level. Considering the proton collision rates in Fig. 4, most 16L2 events which happened at or close to top energy would have resulted in a quench after a few 100 msec if the beams would not have been dumped by the BLMs.

CONCLUSION

Different new phenomena were observed during fast beam loss events in the LHC in 2017, including the possible phase transition of macroparticles (which were presumably the cause of the losses) and rapidly developing beam instabilities. The analysis in this paper indicates that the macroparticle radius must have been of the order of a few tens of μm and that the energy deposition was likely high enough to explain a phase transition. The beam-gas collision rates observed during the subsequent gas phase were sufficient to quench arc dipoles within less than a second if no BLM dump would have occurred. This demonstrates that 16L2 macroparticles would have unavoidably perturbed the machine availability even if no beam instabilities would have developed.

REFERENCES

[1] T. Baer *et al.*, "UFOs in the LHC", in *Proc. 2nd Int. Particle Accelerator Conf. (IPAC'11)*, San Sebastián, Spain, Sep. 2011, paper TUPC137, pp. 1347–1349.

[2] E. Nebot *et al.*, "Analysis of fast losses in the LHC with the BLM system", in *Proc. 2nd Int. Particle Accelerator Conf. (IPAC'11)*, San Sebastián, Spain, Sep. 2011, paper TUPC136, pp. 1344–1346.

[3] T. Baer *et al.*, "UFOs in the LHC: Observations, studies, and extrapolations", in *Proc. 3rd Int. Particle Accelerator Conf. (IPAC'12)*, New Orleans, LA, USA, May 2012, paper THPPP086, pp. 3936–3938.

[4] B. Goddard *et al.*, "Transient beam losses in the LHC injection kickers from micron scale dust particles", in *Proc. 3rd Int. Particle Accelerator Conf. (IPAC'12)*, New Orleans, LA, USA, May 2012, paper TUPPR092, pp. 2044–2046.

[5] T. Baer, "Very Fast Losses of the Circulating LHC Beam, their Mitigation and Machine Protection" Ph.D. Thesis, Hamburg University, 2013.

[6] B. Auchmann, J. Ghini, L. Grob, G. Iadarola, A. Lechner and G. Papotti, "How to survive an UFO attack?", in Proceedings of the 6th Evian Workshop on LHC Beam Operation, Evian Les Bains, France, 2015, pp. 81–86.

[7] G. Papotti *et al.*, "Macroparticle-induced losses during 6.5 TeV LHC operation", in *Proc. 7th Int. Particle Accelerator Conf. (IPAC'16)*, Busan, South Korea, May 2016, paper TUPMW023, pp. 1481–1484.

[8] A. Lechner *et al.*, "BLM Thresholds and UFOs", in *Proc. 7th Evian Workshop on LHC Beam Operation*, Evian Les Bains, France, 2016, pp. 209-214.

[9] L. Mether *et al.*, "16L2: Operation, observations and physics aspects", in *Proc. 7th Evian Workshop on LHC Beam Operation*, Evian Les Bains, France, 2017.

[10] J.M. Jiménez *et al.*, "Observations, Analysis and Mitigation of Recurrent LHC Beam Dumps Caused by Fast Losses in Arc half-cell 16L2", in *Proc. 9th Int. Particle Accelerator Conf. (IPAC'18)*, Vancouver, Canada, Apr-May 2018, paper MOPMF053, this conference.

[11] B. Salvant *et al.*, "Experimental Characterisation of a Fast Instability Linked to Losses in the 16L2 Cryogenic Half-Cell in the CERN LHC", in *Proc. 9th Int. Particle Accelerator Conf. (IPAC'18)*, Vancouver, Canada, Apr-May 2018, paper THPAF058, this conference.

[12] T.T. Böhlen *et al.*, "The FLUKA Code: Developments and Challenges for High Energy and Medical Applications" *Nuclear Data Sheet*s vol. 120, pp. 211-214, 2014.

[13] A. Ferrari, P.R. Sala, A. Fassò, and J. Ranft, "FLUKA: a multi-particle transport code" Rep. CERN-2005-10, 2005, INFN/TC_05/11, SLAC-R-773.

[14] B. Lindstrom *et al.*, "Results of UFO dynamics studies with beam in the LHC", in *Proc. 9th Int. Particle Accelerator Conf. (IPAC'18)*, Vancouver, Canada, Apr-May 2018, paper THYGBD2, this conference.

[15] L. Grob *et al.*, "Analysis of loss signatures of unidentified falling objects in the LHC", in *Proc. 9th Int. Particle Accelerator Conf. (IPAC'18)*, Vancouver, Canada, Apr-May 2018, paper TUPAF049, this conference.

[16] S. Rowan *et al.*, "Interactions between macroparticles and high-energy proton beams", in *Proc. 6th Int. Particle Accelerator Conf. (IPAC'15)*, Richmond, VA, USA, May 2015, paper TUPTY045, pp. 2112–2115.

[17] B. Auchmann *et al.*, "BLM Threshold strategy (vis-a-vis UFOs and quenches)", in *Proc. LHC Performance Workshop*, Chamonix, France, 2014.

[18] A. Verweij, "QP3: Users Manual", CERN/TE, EDMS 1150045, 2008.

[19] B. Auchmann *et al.*, "Testing beam-induced quench levels of LHC superconducting magnets", *Phys. Rev. ST Accel. Beams* vol. 18, p. 061002, 2015.